Quality of protein structural data and radiation damage estimation at beamline 1.3W: SAXS/WAXS

Nuntaporn Kamonsutthipaijit[a,*], **Nongluk Yutaekool**[b], **Siriwat Soontranon**[a], **Supagorn Rugmai**[a]

[a] Synchrotron Light Research Institute (Public Organization), Nakhon Ratchasima 30000 Thailand
[b] School of Biochemistry, Institute of Science, Suranaree University of Technology, Nakhon Ratchasima 30000 Thailand

*Corresponding author, e-mail: nuntaporn@slri.or.th

ABSTRACT: Small Angle X-ray Scattering (SAXS) is a useful technique that can provide structural information in terms of size, shape, and multiple conformations of a protein sample and can also be used to reconstruct a three-dimensional structure in low resolution of a macromolecule. SAXS data were collected and analyzed from a set of nine proteins with MW ranging from 14 to 400 kDa whose crystal structures were available from the PDB. The crystallographic data are used to validate the accuracy of the structure obtained from the SAXS data. By comparing data from both techniques, they can provide good complementary structural information to each other. Interestingly, no radiation damage of protein samples was observed by X-ray exposure at Beamline 1.3W, Synchrotron Light Research Institute, Thailand. This was confirmed with the chromatography technique by comparing the purity of the protein samples before and after SAXS measurements. The absorbed dose of each protein sample has also been calculated to confirm that the value is low enough to prevent damage to the proteins. This experiment has shown that the beamline provides SAXS measurements suitable for the broad range of protein structures in a non-destructive way and benefits the research community especially in the field of biological macromolecules in Southeast Asia and the nearby countries.

KEYWORDS: SAXS, protein structure, radiation damage, synchrotron

INTRODUCTION

SAXS experiments using the high brilliance synchrotron source give advantages in terms of short exposure time and a broad variety of experimental setups for the users at the beamline. There are several synchrotron SAXS dedicated to biological macromolecule applications all over the world such as PETRA III [1] in Germany, Spring-8 [2] in Japan, SSRL [3] in USA and ESRF [4] in France. Nevertheless, in ASEAN, there is only 1.2 GeV Synchrotron in Thailand available for such a technique.

Small and Wide X-ray Scattering (SAXS/WAXS) techniques have been available for users at BL1.3W, Siam Photon Laboratory of Synchrotron Light Research Institute (SLRI), Thailand since 2011. This multipurpose SAXS/WAXS technique provided by the beamline is suitable for a variety of research. SAXS provides information about the size and shape of nanoparticles and nanostructures, while WAXS provides information on the crystalline structure of the samples. At the beginning of the design, X-rays were delivered from a bending magnet (BM) source for the BL1.3W users [5]. Two years later, a 5-period multipole wiggler with an effective magnetic field of 2.2 T was installed. The beamline optics have been modified and relocated to utilize high-intensity x-ray from the multipole wiggler [6]. Since then, BL1.3W: SAXS/WAXS has been in operation and welcoming users from around the world especially in ASEAN. To serve the growing macromolecular research community, the capability of the

station has also been expanded to BioSAXS technique.

Apart from the interpretation of SAXS data following the publication guideline [7], the validation of data with other synchrotrons can also show the performance of the beamline. Owing to the recommendations from the SASvtf report [8], small-angle scattering experimental data and model data bank (SASBDB) accessible via https://www.sasbdb.org [9] have been developed with respect to model validation and archiving. This system is a federated system of the data bank to promote the propagation and validation of scattering data and models, which are publicly accessible. 93% of the deposited scattering data were measured by synchrotron radiation facilities, and the rest were from other sources (in-house or neutron) [10]. This allows us to freely access and download the experimental SAXS data and compare the SAXS data from different synchrotrons with publication-level quality.

Under the intense X-ray beam from a synchrotron source, samples can undergo the formation of aggregates that are caused by radiation damage. In principle, the mechanism of radiation damage starts from the photolysis of water in the supporting solvent which generates free hydroxyl and hydroperoxyl radicals, and then those radicals continuously activate the polypeptide chain of proteins, driving the formation of aggregates [11]. There are several strategies to reduce the damage including sample-flow experiment or translating sample cell [12], beam attenuation [13], beam defocusing and reduction of sample exposure

time. Some of these methods compromise the quality of data, and some come with complicated operation at facilities and expensive costs. Aside from that, an easier way to control the effect of radiation damage is the addition of small molecules such as dithiothreitol (DTT) [13] and glycerol [13, 14] to the protein solution. The last method, however, also reduced signal-to-noise ratios in the collected data as shown in the case of adding glycerol [13]. It is necessary to evaluate the absorbed dose of the proteins in a wide range of molecular weight at BL1.3W to ensure that the users of the beamline can control the radiation damage with suitable strategies during the SAXS experiment.

In this paper, the information obtained from SAXS on a set of nine proteins with molecular weight in a range of 14 to 400 kDa whose crystallographic information is available is described. We demonstrate how information from SAXS complements the high-resolution structural information from crystallography in terms of scattering curves and the three-dimensional molecular envelopes. Moreover, the radiation damage has been manually evaluated both from the theoretical equation and from the RADDOSE-3D software in order to estimate the radiation doses of the nine different proteins in the SAXS experiments. The latter method can reduce the burden of manually performing the calculation. This can ensure the users that their protein will absorb the dose lower than the limitation of radiation damage from this beamline setup.

MATERIALS AND METHODS

Sample preparation

Proteins, chicken egg-white lysozyme (product number (PN)-62971), myelin basic protein (MBP) (PN-M1891), chymotrypsinogen A (PN-C4879), and BSA (PN-05470), were purchased from Sigma-Aldrich. Carbonic anhydrase, β-amylase, and apoferritin were part of the kit for molecular weights of 29–700 kDa from Sigma-Aldrich (PN-MWGF1000). Ovalbumin and aldolase were part of gel-filtration calibration kits from GE Healthcare (PN-28403842). All proteins except apoferritin were in powder form and were dissolved in dialysis overnight after dissolving. MBP and apoferritin were freshly dissolved into the appropriate buffer before SAXS experiments without dialysis. The buffers used were 100 mM Tris 100 mM NaCl, pH 7.5 for all proteins except lysozyme (40 mM acetic acid 50 mM NaCl pH 4.0) and BSA (50 mM HEPES pH 7.5). The final concentrations were determined by a Nanodrop ND-1000 spectrophotometer. The extinction coefficients of the proteins were calculated using the online tool ProtParam [15].

SAXS data collection

SAXS data from the protein samples were collected at Beamline 1.3W of Synchrotron Light Research Institute (Public Organization), Thailand. The SAXS intensity data ($I(q)$ versus q, where $q = (4\pi \sin\theta)/\lambda$, 2θ is the scattering angle, and λ is the X-ray wavelength), were obtained at a photon flux of 2.7×10^9 photons/s at 9 keV ($\lambda = 0.138$ nm) using a three-pair slit collimated incident beam with a maximum dimension of 1500 (Horizontal) µm × 1000 (Vertical) µm at the sample position. Samples were injected into the sample cell, which was made of copper blocks with PTFE insertion (0.15 cm thickness) and 60-µm-thick Kapton tapes as windows. The sample cell volume required is 60 µl in air. Data were collected in static sample mode using a Rayonix SX165 CCD detector.

Before data collection, the samples were centrifuged at 10 000 rpm at 4 °C for 600 s to remove any aggregates. The samples were then exposed to X-ray at 16 °C for 600 s. After dialysis, the concentration of the samples was diluted to a series of 2, 3, and 5 mg/ml for proteins with MW > 50 kDa (except aldolase, only 3 and 5 mg/ml) and a series of 5, 7, and 10 mg/ml for proteins with MW < 50 kDa (except MBP, only 5.5 and 7.6 5 mg/ml). The sample-to-detector distance (SDD) was set into three groups of proteins which were 1200 mm for lysozyme, chymotrypsinogen A, and carbonic anhydrase, 2200 mm for ovalbumin, BSA, aldolase, β-amylase, and MBP, and 4300 mm for apoferritin. This enabled us to capture SAXS data with the three sets of q range of 0.0444–0.5148 Å^{-1}, 0.0252–0.3222 Å^{-1}, and 0.0128–0.1534 Å^{-1}, respectively. The empty sample cell was measured first, followed by the matched reference buffer, and then the protein sample. Protein samples before and after SAXS experiments were collected to check the formation of aggregates using High-Performance Liquid Chromatography (HPLC). By HPLC analysis, all protein samples before and after exposure to the X-ray from SAXS experiments were determined by using the silica columns (Shimadzu), consisting of Shodex protein KW-802.5 connected with KW-804 with an HPLC system (Shimadzu). All proteins were eluted with 100 mM Tris 100 mM NaCl, pH 7.5 at a constant flow rate of 1.0 ml/min. The absorbance at 280 was monitored for the proteins.

SAXS data analysis

The raw data were processed by standard procedures using the program SAXSIT, which was developed by Beamline 1.3W and BioXTAS RAW [16], to obtain SAXS curves. The radius of gyration, R_g of each protein was evaluated using Guinier approximation assuming that at $q < 1.3R_g$; the intensity is represented as $I(q) = I(0)\exp[-(qR_g)^2/3]$. In addition, R_g and the maximum dimension of the protein, D_{max}, and the pair distribution function, $P(r)$ were computed using GNOM program [17] which is part of the AT-SAS package version 3.0 [18]. Both R_g and D_{max} of each protein were extracted from Guinier and $P(r)$, respectively. The results were compared to those

from its corresponding proteins which are deposited in SASBDB [9] as the accession number listed here: SASAC2 (lysozyme), SASDDF6 (MBP), SASAA8 (chymotrypsinogen A), SASDA78 (carbonic anhydrase), SASDE35 (ovalbumin), SASDA32 (BSA), SASDA68 (aldolase), SASDA62 (β-amylase), and SASDA82 (apoferritin). All SASBDB benchmark data are selected from the synchrotron SAXS measurements with the same types of proteins and buffer conditions. To validate the SAXS data, the comparison between experimental scattering curves of the proteins with the highest concentration and the known high-resolution models from crystal structures taken from the Protein Data Bank (PDB) [19] was carried out using CRYSOL [20] from the ATSAS package. The *ab initio* reconstructions of the low-resolution particle envelopes were performed from the SAXS data of the highest concentration of the proteins using the DAMMIF server [21] without imposed symmetry (P1) and 20 independent models. Each average reconstruction was aligned with its corresponding atomic structure from PDB using SUPALM in SASREF [22] plugin and visualized using PyMOL version 2.4.1. The PDB codes of the crystallographic models are 1LYZ (lysozyme), 2CGA (chymotrypsinogen A), 1V9E (carbonic anhydrase), 1OVA (ovalbumin), 3V03 (BSA), 1ZAH (aldolase), 1FA2 (β-amylase), and 1IER (apoferritin). For MBP, there is no high-resolution model available, and thus it is overlaid with the SASBDB model in reference [23] instead.

Absorbed dose estimation

The absorbed dose, *D*, in Gy, is the X-ray dose delivered to the sample which was calculated using the finite path length of the sample from Eq. (1) [13, 24] as

$$D = \frac{1000Etf}{\rho_m A L}\left[1 - \frac{1}{\exp(\mu \rho_m L/\rho)}\right] \qquad (1)$$

where E is the X-ray energy per photon (J/photon), t is the exposure time (s), f is the beam flux (photons/s) which passed through the sample and transmitted to the first 60 μm Kapton window of the sample cell with the mass density of Kapton to be 1.42 g/cm³. The Kapton transmission was calculated using the X-ray Optics server via http://henke.lbl.gov/optical_constants/filter2.html [25]; A (cm²) is the total beam area, and L (cm) is the sample pathlength or thickness which corresponds to the size of the sample cell of 0.15 cm. For each protein sample, the mass density, ρ_m (g/cm³), was evaluated using MULCh [26], and the atomic formular was obtained from ProtParam [15] while the average mass attenuation coefficient, μ/ρ (cm²/g), was calculated without coherent scattering by the XCOM Photon Cross Sections Database via http://www.nist.gov/pml/data/xcom/index.cfm [27]. The Gy unit of the absorbed dose was obtained by factor 1000 which converts J/g into J/kg. For further information is described in the supporting data
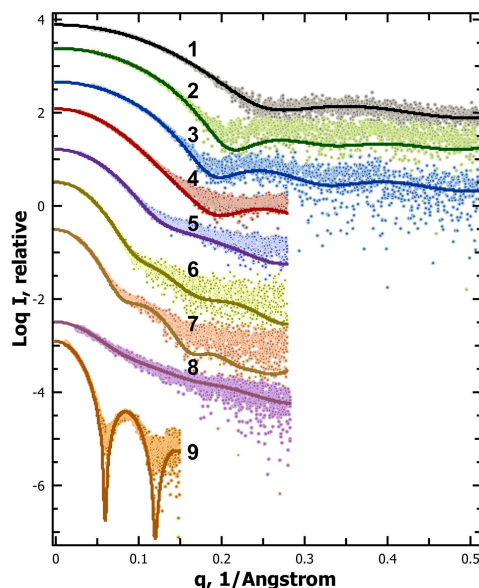
Fig. 1 The experimental scattering curves (dots) and structural fits (solid line). The fits are from the crystallographic models generated by CRYSOL [20]. The logarithm of $I(q)$ (a.u.) as a function of q (Å⁻¹) was plotted, vertically offset for clarity. (1) lysozyme, (2) chymotrypsinogen A, (3) carbonic anhydrase, (4) ovalbumin, (5) BSA, (6) aldolase, (7) β-amylase, (8) MBP, and (9) apoferritin.

(Tables S1–S3). In parallel, the estimation of absorbed dose is also computed by RADDOSE-3D software version 4.0 [28] to compare with those calculated from the above equation using the same beamline parameter as described in the supporting data (Tables S1–S3).

RESULTS AND DISCUSSION

Quality of structural data from SAXS

SAXS data of the nine protein samples were collected at Beamline 1.3W (see supporting data (Figs. S1–S9) for the scattering graphs of each protein) and were analyzed as summarized in Table 1. In Guinier approximation, the R_g derived ranging from lysozyme to apoferritin were obtained from 13 to 75 Å, respectively, while $P(r)$ analysis provided the D_{max} in the range of 39 to 255 Å, respectively. The differences in the R_g and the D_{max} in the protein samples between the experimental and the previously reported in SASBDB [9] were small and within the average deviation of less than 1.6 Å and 3.3 Å, respectively (Table 1). The MWs of all proteins were calculated in the range from 11 to 592 kDa. There was relatively good agreement between the MW of the theory and that calculated from SAXS data using the volume of correlation method [29] with the average errors of about 20% (Table 1). The higher the concentration used to calculate the MW with the correlation method, the less the deviation of the

Table 1 All R_g, D_{max}, and MW from Guinier approximation, $P(r)$ analysis, and the volume of correlation method [29], respectively, for the protein samples in comparison to those from their corresponding SASBDB.

| Sample	Conc.	Guinier (Å)			$P(r)$ analysis (Å)			Calculated	
(MW$_{theor.}$, kDa)	(mg/ml)	R_g	$R_{g,SASBDB}$	%ΔR_g	D_{max}	$D_{max,SASBDB}$	%ΔD_{max}	MW (kDa)	%ΔMW
Lysozyme (14)	5.0	14		−7	44		10	11	23
	7.0	14	15	−9	39	40	−2	11	21
	10.0	13		−12	39		−2	11	24
MBP (18)	5.5	27	33	−18	104	111	−6	15	16
	7.6	30		−10	108		−3	21	−19
Chymotrypsinogen A (26)	5.0	18		−7	49		−2	18	31
	7.0	18	19	−7	48	50	−4	16	39
	10.0	18		−7	50		0	18	31
Carbonic anhydrase (33)	5.0	20		−6	60		0	25	13
	7.0	20	21	−5	60	60	0	24	17
	10.0	20		−6	63		5	23	20
Ovalbumin (40)	5.0	26		9	82		5	43	0
	7.0	26	24	9	84	78	8	42	1
	10.0	25		5	83		6	41	4
BSA (44)	2.0	29		−1	89		−4	48	31
	3.0	28	29	−3	88	93	−5	52	25
	5.0	28		−2	93		0	55	21
Aldolase (157)	3.0	36	36	0	103	105	−2	134	15
	5.0	36		0	106		1	135	14
β-Amylase (162)	2.0	43		2	122		−4	134	40
	3.0	43	42	1	126	127	−1	130	42
	5.0	43		3	129		2	162	28
Apoferritin (479)	2.0	62		−9	135		6	806	−68
	3.0	63	68	−7	138	128	8	540	−13
	5.0	68		1	136		6	592	−24

%Δ describes the difference of R_g and D_{max} values between experimental and SASBDB and MW between the calculated and theory. The SASBDB codes of each protein are provided in the materials and methods part. The SAXS analysis from SASBDB data that is taken for the benchmark is from one concentration.

MW to the one from the theory when comparing in the same protein, which is attributed to the better signal to noise ratio of the scattering data.

Fig. 1 shows representative scattering curves of the proteins and the theoretical patterns computed from the available crystallographic models of the same or of highly homologous proteins taken from the Protein Data Bank [19]. The PDB codes of the crystallographic models are presented in Fig. 1 legend (no homologous structure is available for MBP). The fits to the curves calculated from the crystallographic models are rather good, which means that the crystal structure or oligomeric composition of the protein in the crystal agrees well with that in solution although β-amylase (sample 7 in Fig. 1) looks less well fit when compared to the other proteins at a high q-range (above 0.15 Å^{-1}). This might be from the effect of background matching during the SAXS experiment. The quality of the fit between both techniques was indicated by an error-weighted residual difference plot of $\Delta/\sigma = [I_{exp}(q) - cI_{mod}(q)]/\sigma(q)$ versus q (shown

in the lower panel in supporting data (Figs. S1–S9) of CRYSOL plot in each protein) that is relatively evenly distributed around 0 for all cases. The χ^2 is not considered for this analysis because it is higher than expected, but on inspection, the reduction in BioXTAS RAW did not provide the error output from a Poisson distribution and then was low estimates of the variation in the data [16], which leads to the artificially high χ^2. Regarding the *ab initio* molecular envelopes, there is a good correlation with all the envelopes and the crystallographic models as seen in Fig. 2, which corresponds to the scattering curve overlaid with the one computed from PDB code in Fig. 1. The known structure is shown in a ribbon form for clarity, and the empty space in the envelope can be occupied with the side chain in the protein structure.

With all results from the overall parameters (i.e., R_g, D_{max}, and MW), validated SAXS data to the known model, and reconstructed 3D molecular envelopes, it has shown that the quality of SAXS data performed at BL1.3W is in very good agreement to the other
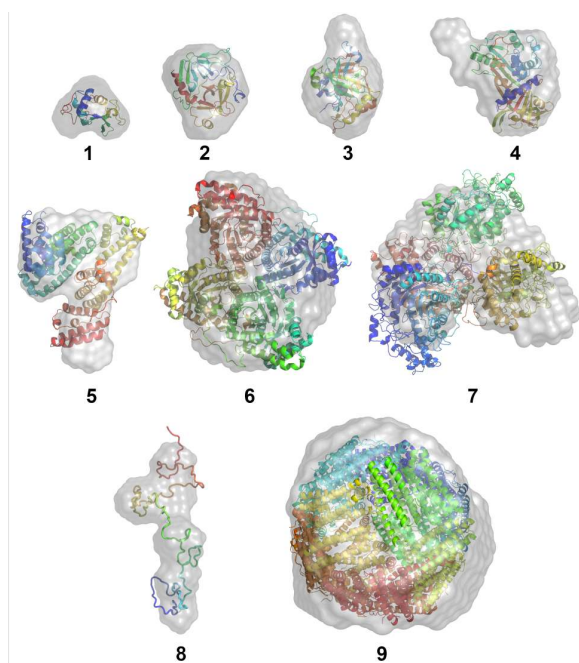
Fig. 2 The *ab initio* SAXS derived envelopes (gray surface) superimposed with crystallographic structures (ribbon) are illustrated in the agreement between SAXS and crystallography techniques. (1) lysozyme, (2) chymotrypsinogen A, (3) carbonic anhydrase, (4) ovalbumin, (5) BSA, (6) aldolase, (7) β-amylase, (8) MBP, and (9) apoferritin.

Table 2 Estimation of absorbed dose calculated at Beamline 1.3W.

Sample	Conc. (mg/ml)	Absorbed dose (Gy) from Eq. (1)[a]
Lysozyme	5.0	679.9
	7.0	679.8
	10.0	679.6
MBP	5.5	680.4
	7.6	680.1
Chymotryp- sinogen A	5.0	680.6
	7.0	680.5
	10.0	680.1
Carbonic anhydrase	5.0	680.5
	7.0	680.2
	10.0	679.8
Ovalbumin	5.0	680.7
	7.0	680.5
	10.0	680.2
BSA	2.0	679.8
	3.0	679.7
	5.0	679.6
Aldolase	3.0	680.8
	5.0	680.6
β-Amylase	2.0	680.9
	3.0	680.8
	5.0	680.6
Apoferritin	2.0	680.9
	3.0	680.8
	5.0	680.6

[a] Absorbed dose calculated using the equation from previous research [13] as described in Materials and Methods section and the supporting data (Tables S1–S3). RADDOSE-3D [28] provides the results in 0.000753 MGy with six decimal points for all proteins.

synchrotrons with an insignificant deviation of data.

Radiation damage of protein

Sample purity before and after doing SAXS was monitored using HPLC, and no change was found in the chromatogram (the result shown in the supporting data (Figs. S10–S11)) which can be an indication that there is no radiation damage to the protein sample performed at the BL1.3W without sample flow measurement. This leads to the interest in the absorbed dose that might occur in the SAXS experiment to the protein samples. In this study, we estimated the absorbed dose from the equation previously reported [13] and RADDOSE-3D software [28]. When the static protein is exposed to X-ray at BL1.3W, the absorbed dose calculated from Eq. (1) ranges from 679.2 to 680.9 Gy (Table 2), while RADDOSE-3D provides the results in 0.000753 MGy or 753 Gy with six decimal points for all proteins. When compared the value of absorbed dose calculated by Eq. (1) in the same protein with different concentrations, it was found that at the lower concentration, the absorbed dose is higher, which corresponds to the previous research [13]. The variation of the absorbed dose from Eq. (1) in each protein is attributed to the different protein molecular weight, concentration, and buffer composition. The absorbed

doses derived from Eq. (1) and RADDOSE-3D are in good agreement even though in latter did not take the buffer composition into account. This might be because there was no presence of heavy atoms in the solvent.

According to the previous research on the limitation of radiation damage, proteins with greater molecular weight can survive the X-ray with the greater critical dose as seen in the change in R_g at higher absorbed dose [13]. In our study, lysozyme absorbed radiation dose about 680 Gy and 753 Gy calculated from Eq. (1) and RADDOSE-3D, respectively. These values are higher than the critical dose of lysozyme found from other SAXS experiments at other synchrotrons which are around 400 Gy from Spring-8 [14] and 293–365 Gy from PETRAIII [13]. However, we did not observe the formation of aggregates from HPLC, nor change in the radius of gyration upon increasing concentration. This might be reasoned from the beam

area [1500 (Horizontal) µm × 1000 (Vertical) µm] of BL1.3W which is twice larger than those from the SAXS setups at Spring-8 [800 (Horizontal) µm × 600 (Vertical) µm] [14] and PETRAIII [500 (Horizontal) µm × 250 (Vertical) µm] [13]. Thus, the radiation at BL1.3W is evenly distributed within the beam area. Had the aggregation been noticed, X-ray exposure time of the SAXS experiment at BL1.3W could have been reduced from 600 s to limit the radiation damage while the quality of data was maintained. Although the larger beam of our beamline could minimize the radiation damage during the experiments, the trade-off would be the longer exposure time (approximately 10 min for each experiment) and the need for a higher concentration of the protein than the measurements conducted at other high-brightness synchrotrons. This can make some difficulties in some beamline setups such as flow sample experiments (e.g., coupling of chromatography with SAXS) in which a large volume of sample is required.

Although the absorbed dose calculated for BL1.3W is quite low to form the aggregates, this issue should be taken into account to optimize the experiment and get successful data collection. There are many ways to cope with the radiation damage at the beamline, and the most commonly used and straightforward to the users are solution additives. The addition of either glycerol, ascorbic acid, or DTT effectively decreases the radiation damage [13, 14, 30]. They can be added for different purposes. For example, glycerol is added for stabilization while DTT is the reducing agent which can reduce disulfide bonds of protein to avoid aggregation. However, one must keep in mind that doping a sample with the solution additives can make undesirable changes in the protein structure as well. Each additive has its different disadvantages. For instance, apart from the short shelf-life of DTT, it can absorb UV at 280 nm, resulting in misleading the estimation of protein concentration [31]. Glycerol makes difficulty in pipetting, and more importantly, it reduces the contrast of a sample. If too much excess is added, the interaction between protein itself or between protein and solvent may happen, leading to the disruption of the oligomeric states [32]. However, it would be best not to use any solvent additive approach that will change the solvent environment of the sample, leading to the increasing risk of altering the structural properties of a protein if the beamline has low risk of radiation damage like BL1.3W and can already deliver qualitative SAXS data.

CONCLUSION

Here, the quality of SAXS data and radiation damage calculation that BioSAXS users of BL1.3W: SAXS/WAXS will obtain have been described and compared to the other synchrotron SAXS/WAXS facilities. We show that the R_g, D_{max}, and MW analyzed from

qualitative SAXS data of the proteins with molecular weights ranging from 14 to 400 kDa have the deviations from the SAXS data deposited in SASBDB of less than 1.6 Å (R_g) and 3 Å (D_{max}) and MW with error of about 20%. The fits of the scattering curves and their reconstructions of three-dimensions to the ones computed from the crystallographic structures are rather good, which confirms that BL1.3W has a capability to deliver SAXS information in complementary to high-resolution structural techniques. The absorbed dose generated from this beamline is relatively lower than the threshold of the radiation damage, so there is no need to add any scavenger additives into the sample to prevent the damage unless the proteins from the users are very sensitive to X-ray in which the additives can be considered on a case-by-case basis.

Appendix A. Supplementary data

Supplementary data associated with this article can be found at http://dx.doi.org/10.2306/scienceasia1513-1874. 2022.064.

REFERENCES

1. Gräwert TW, Svergun DI (2020) Structural modeling using solution small-angle X-ray scattering (SAXS). *J Mol Biol* **432**, 3078–3092.
2. Fujisawa T, Inoue K, Oka T, Iwamoto H, Uruga T, Kumasaka T, Inoko Y, Yagi N, et al (2000) Small-angle X-ray scattering station at the SPring-8 RIKEN beamline. *J Appl Crystallogr* **33**, 797–800.
3. Martel A, Liu P, Weiss TM, Niebuhr M, Tsuruta H (2012) An integrated high-throughput data acquisition system for biological solution X-ray scattering studies. *J Synchrotron Radiat* **19**, 431–434.
4. Pernot P, Round A, Barrett R, De Maria Antolinos A, Gobbo A, Gordon E, Huet J, Kieffer J, et al (2013) Upgraded ESRF BM29 beamline for SAXS on macromolecules in solution. *J Synchrotron Radiat* **20**, 660–664.
5. Soontaranon S, Rugmai S (2012) Small angle X-ray scattering at Siam Photon Laboratory. *Chin J Phys* **50**, 204–210.
6. Phinjaroenphan R, Soontaranon S, Chirawatkul P, Chaiprapa J, Busayaporn W, Pongampai S, Lapboonreung S, Rugmai S (2013) SAXS/WAXS capability and absolute intensity measurement study at the SAXS beamline of the Siam Photon Laboratory. *J Phys Conf Ser* **425**, ID 132019.
7. Trewhella J, Duff AP, Durand D, Gabel F, Mitchell J, Hendrickson WA, Hura GL, Jacques DA, et al (2017) Publication guidelines for structural modelling of small-angle scattering data from biomolecules in solution: An update research papers. *Acta Cryst D* **73**, 710–728.

8. Trewhella J, Hendrickson WA, Kleywegt GJ, Sali A, Sato M, Schwede T, Svergun DI, Tainer JA, et al (2013) Report of the wwPDB small-angle scattering task force: Data requirements for biomolecular modeling and the PDB. *Structure* **21**, 875–881.

9. Valentini E, Kikhney AG, Previtali G, Jeffries CM, Svergun DI (2015) SASBDB, a repository for biological small-angle scattering data. *Nucleic Acids Res* **43**, D357–D363.

10. Kikhney AG, Borges CR, Molodenskiy DS, Jeffries CM, Svergun DI (2020) SASBDB: Towards an automatically curated and validated repository for biological scattering data. *Protein Sci* **29**, 66–75.

11. Garrison WM (1978) Reaction mechanisms in the radiolysis of fats: A review. *Chem Rev* **87**, 381–398.

12. Fischetti RF, Rodi DJ, Mirza A, Irving TC, Kondrashkina E, Makowski L (2003) High-resolution wide-angle X-ray scattering of protein solutions: Effect of beam dose on protein integrity. *J Synchrotron Radiat* **10**, 398–404.

13. Jeffries CM, Graewert MA, Svergun DI, Blanchet CE (2015) Limiting radiation damage for high-brilliance biological solution scattering: Practical experience at the EMBL P12 beamline PETRAIII. *J Synchrotron Radiat* **22**, 273–279.

14. Kuwamoto S, Akiyama S, Fujisawa T (2004) Radiation damage to a protein solution, detected by synchrotron X-ray small-angle scattering: dose-related considerations and suppression by cryoprotectants. *J Synchrotron Radiat* **11**, 462–468.

15. Gasteiger E, Hoogland C, Gattiker A, Duvaud S, Wilkins MR, Appel RD, Bairoch A (2005) Protein identification and analysis tools on the ExPASy Server. In: Walker JM (ed) *The Proteomics Protocols Handbook*, Humana Press, pp 571–607.

16. Hopkins JB, Gillilan RE, Skou S (2017) BioXTAS RAWâĂŕ: improvements to a free open-source program for small-angle X-ray scattering data reduction and analysis. *J Appl Crystallogr* **50**, 1545–1553.

17. Petoukhov MV, Franke D, Shkumatov AV, Tria G, Kikhney AG, Gajda M, Gorba C, Mertens HDT, et al (2012) New developments in the ATSAS program package for small-angle scattering data analysis. *J Appl Crystallogr* **45**, 342–350.

18. Manalastas-Cantos K, Konarev PV, Hajizadeh NR, Kikhney AG, Petoukhov MV, Molodenskiy DS, Panjkovich A, Mertens HDT, et al (2021) ATSAS 3.0: Expanded functionality and new tools for small-angle scattering data analysis. *J Appl Crystallogr* **54**, 343–355.

19. Bernstein FC, Koetzle TF, Williams GJB, Meyer EF, Brice MD, Rodgers JR, Kennard O, Shimanouchi T, et al (1978) The protein data bank: A computer-based archival file for macromolecular structures. *Arch Biochem Biophys* **185**, 584–591.

20. Svergun D, Barberato C, Koch MHJ (1995) CRYSOL, a program to evaluate X-ray solution scattering of biological macromolecules from atomic coordinates. *J Appl Cryst* **28**, 768–773.

21. Franke D, Svergun DI (2009) DAMMIF, a program for rapid ab-initio shape determination in small-angle scattering. *J Appl Crystallogr* **42**, 342–346.

22. Petoukhov MV, Svergun DI (2005) Global rigid body modeling of macromolecular complexes against small-angle scattering data. *Biophys J* **89**, 1237–1250.

23. Stadler AM, Stingaciu L, Radulescu A, Holderer O, Monkenbusch M, Biehl R, Richter D (2014) Internal nanosecond dynamics in the intrinsically disordered myelin basic protein. *J Am Chem Soc* **136**, 6987–6994.

24. Meisburger SP, Warkentin M, Chen H, Hopkins JB, Gillilan RE, Pollack L, Thorne RE (2013) Breaking the radiation damage limit with cryo-SAXS. *Biophys J* **104**, 227–236.

25. Henke BL, Gullikson EM, Davis JC (1993) X-ray interactions: Photoabsorption, scattering, transmission and reflection at $E = 50$–$30{,}000$ eV, $Z = 1$–92. *At Data Nucl Data Tables* **54**, 181–342.

26. Whitten AE, Cai S, Trewhella J (2008) MULCh: Modules for the analysis of small-angle neutron contrast variation data from biomolecular assemblies. *J Appl Crystallogr* **41**, 222–226.

27. Berger MJ, Hubbell JH, Seltzer SM, Chang J, Coursey JS, Sukumar R, Zucker DS, Olsen K (2010) *XCOM: Photon Cross Section Database*, National Institute of Standards and Technology, Gaithersburg, MD, USA.

28. Brooks-Bartlett JC, Batters RA, Bury CS, Lowe ED, Ginn HM, Round A, Garman EF (2016) Development of tools to automate quantitative analysis of radiation damage in SAXS experiments. *J Synchrotron Radiat* **24**, 63–72.

29. Rambo RP, Tainer JA (2013) Accurate assessment of mass, models and resolution by small-angle scattering. *Nature* **496**, 477–481.

30. Jacques DA, Trewhella J (2010) Small-angle scattering for structural biology: Expanding the frontier while avoiding the pitfalls. *Protein Sci* **19**, 642–657.

31. Grishaev A (2012) Sample preparation, data collection, and preliminary data analysis in biomolecular solution X-ray scattering. *Curr Protoc Protein Sci* **1**, 1–18.

32. Vagenende V, Yap MGS, Trout BL (2009) Mechanisms of protein stabilization and prevention of protein aggregation by glycerol. *Biochemistry* **48**, 11084–11096.

Appendix A. Supplementary data

Table S1 Beam dimension of beamline 1.3W.

Beam parameter	Dimension
Horizontal (cm)	0.15
Vertical (cm)	0.10
Area (cm^2)	0.015

Table S2 Liquid cell dimension of beamline 1.3W.

Liquid cell	Dimension
Horizontal (cm)	1.0
Vertical (cm)	0.4
Sample cell thickness[*](cm^2)	0.15

[*] Used as the sample pathlength, L, for Gy calculation.

Table S3 Beam flux and energy parameters of beamline 1.3W.

Beam parameter	Value
Beam flux (photon/s)	2.70×10^9
Liquid cell wall transmission[*]	0.9657
Sample flux (photon/s)[**]	2.61×10^9
λ (m)[***]	1.38×10^{-10}
Energy per photon (J/photon)[***]	1.44×10^{-15}
Energy delivered to sample per s (J/s)	3.7626×10^{-6}
Energy delivered to sample per s per unit beam area (J/s/cm^2)	2.5084×10^{-4}

[*] Kapton wall transmission is calculated from polyimide 60 μm with a mass density, $\rho_m = 1.42$ g/cm^3.

[**] The flux is considered as it passed through the sample and transmitted to the first 60 μm Kapton window of the sample cell.

[***] λ is wavelength in m unit and energy per photon (J/photon0) is calculated from $E = hc/\lambda$, where $\lambda = 1.3776$ Å or 9 keV and h is Plank's constant, while c is the speed of light.
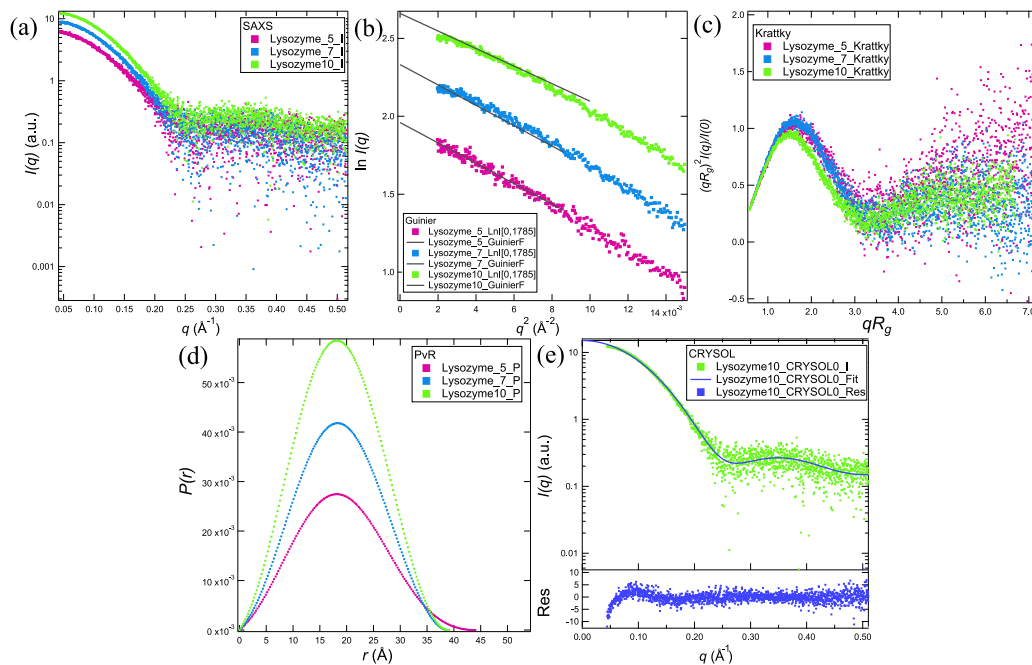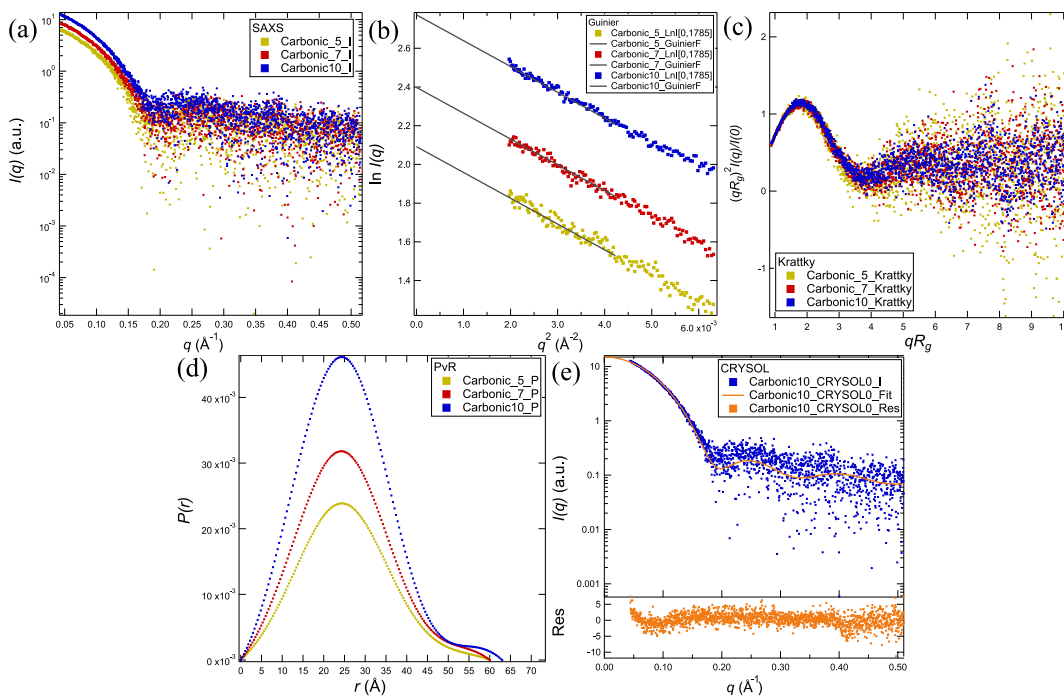
Fig. S1 (a) SAXS patterns of lysozyme in the concentrations of 5, 7 and 10 mg/ml (pink, blue and green, respectively). (b) Guinier plots (black line indicates the fitting). (c) Kratky plots and (d) $P(r)$. (e) Experimental scattering (dots) and the fit from PDB entry 1LYZ (solid line).
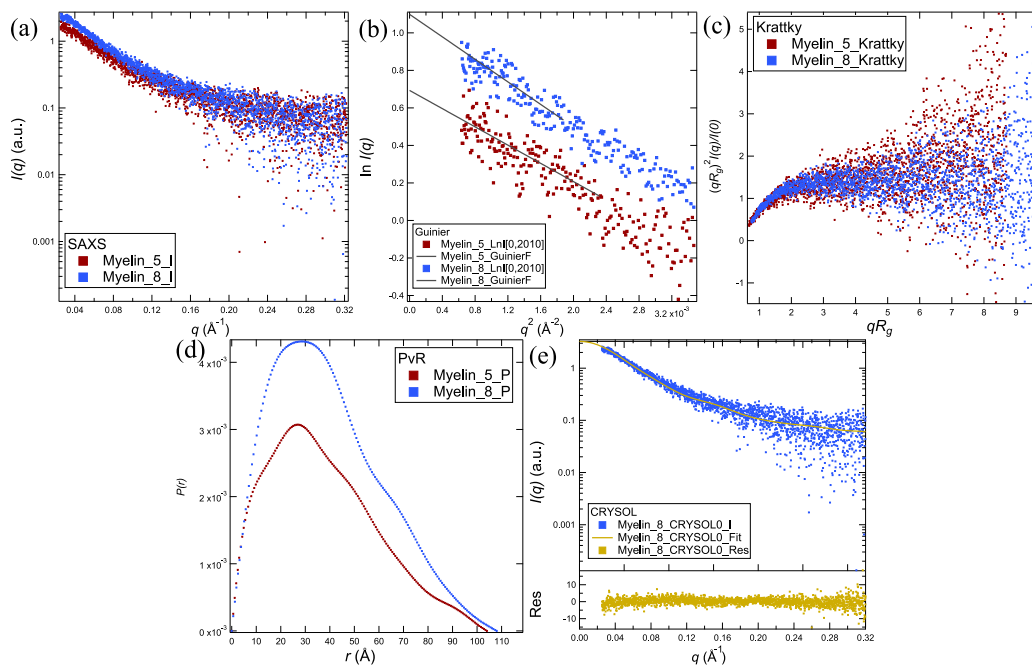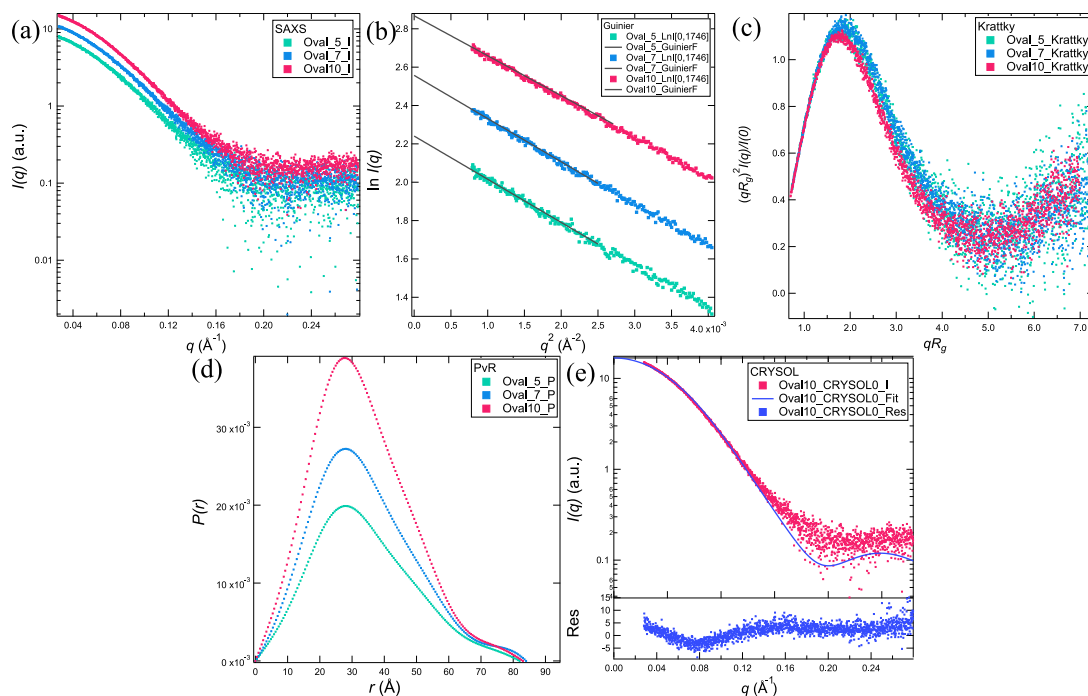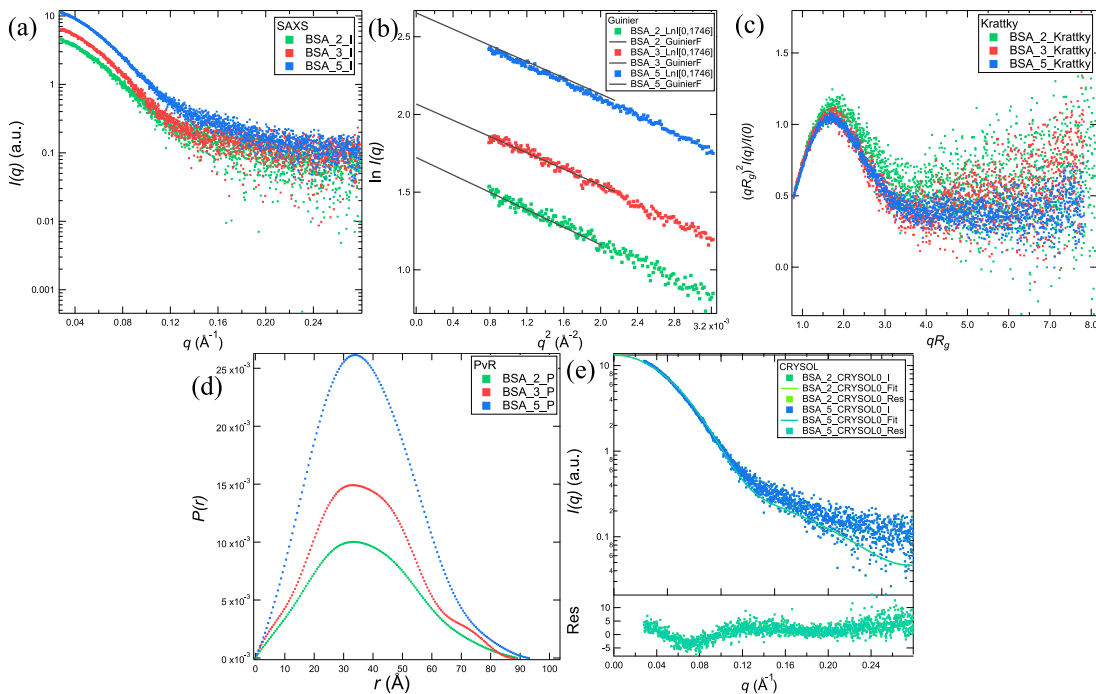

Fig. S2 (a) SAXS patterns of MBP in the concentrations of 5.5 and 7.6 mg/ml (red and blue, respectively). (b) Guinier plots (black line indicates the fitting). (c) Kratky plots and (d) $P(r)$. (e) Experimental scattering (dots) and the fit from SASBDB entry SASDDF6 (solid line).
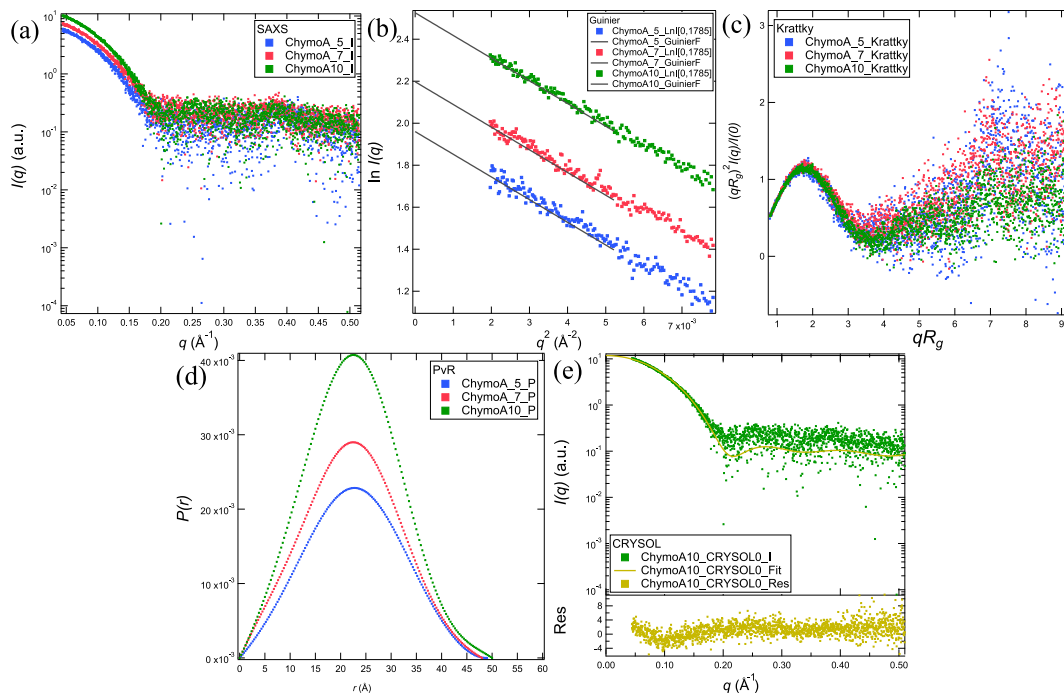
Fig. S3 (a) SAXS patterns of chymotrypsinogen A in the concentrations of 5, 7 and 10 mg/ml (blue, red and green, respectively). (b) Guinier plots (black line indicates the fitting). (c) Kratky plots and (d) $P(r)$. (e) Experimental scattering (dots) and the fit from PDB entry 2CGA (solid line).
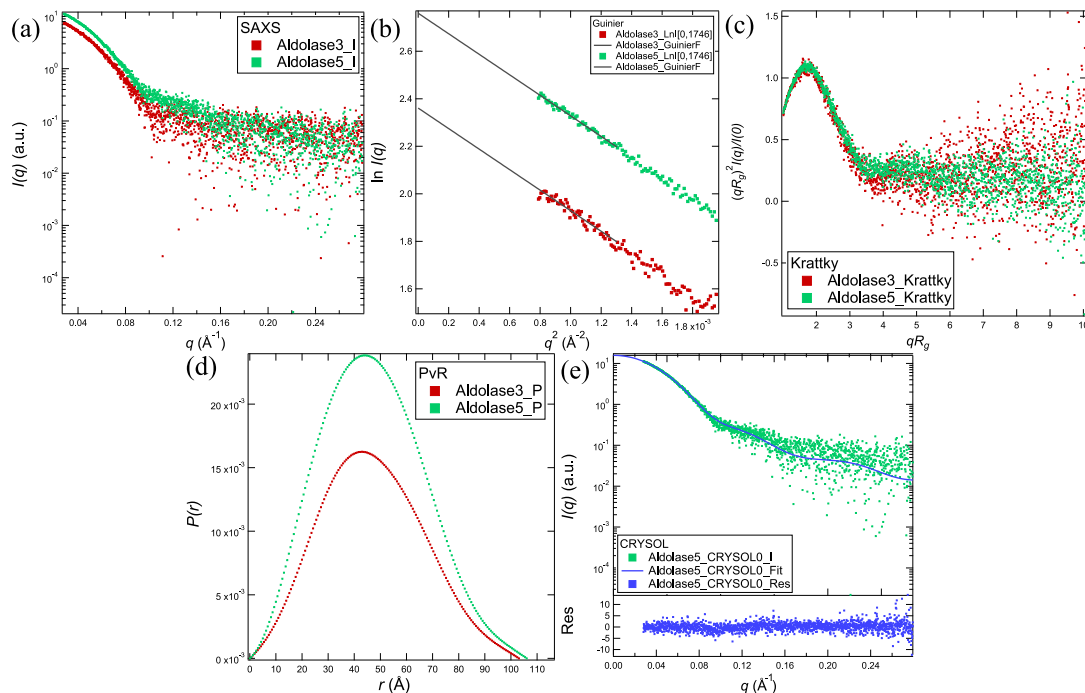

Fig. S4 (a) SAXS patterns of carbonic anhydrase in the concentrations of 5, 7 and 10 mg/ml (yellow, red and blue, respectively). (b) Guinier plots (black line indicates the fitting). (c) Kratky plots and (d) $P(r)$. (e) Experimental scattering (dots) and the fit from PDB entry 1V9E (solid line).
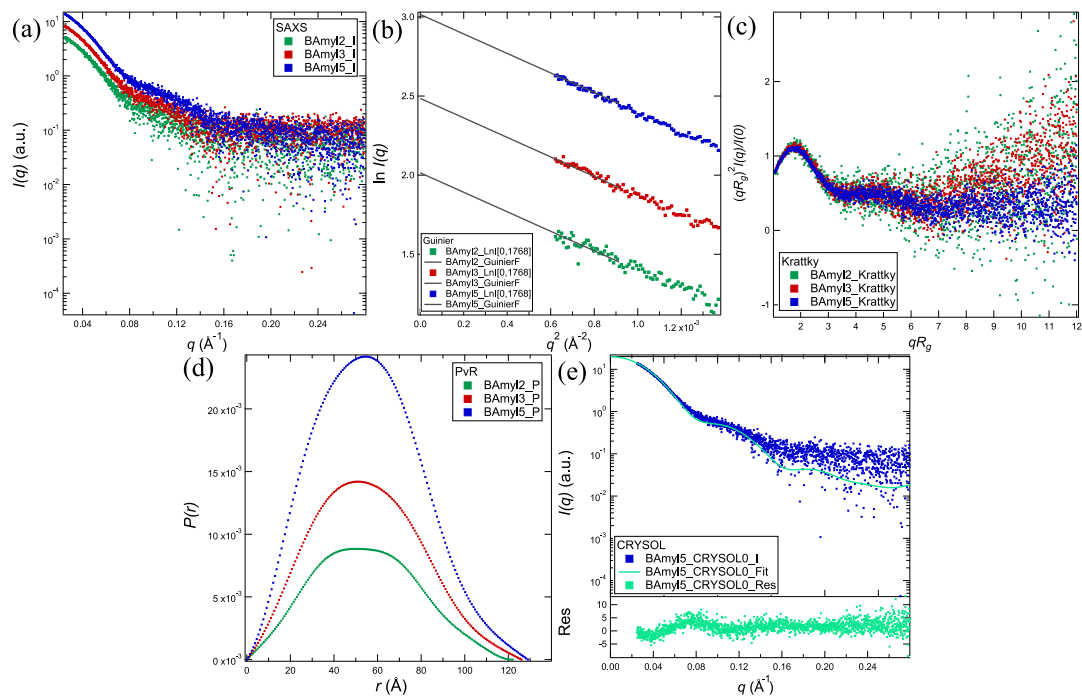
Fig. S5 (a) SAXS patterns of ovalbumin in the concentrations of 5, 7 and 10 mg/ml (green, blue and red, respectively). (b) Guinier plots (black line indicates the fitting). (c) Kratky plots and (d) $P(r)$. (e) Experimental scattering (dots) and the fit from PDB entry 1OVA (solid line).
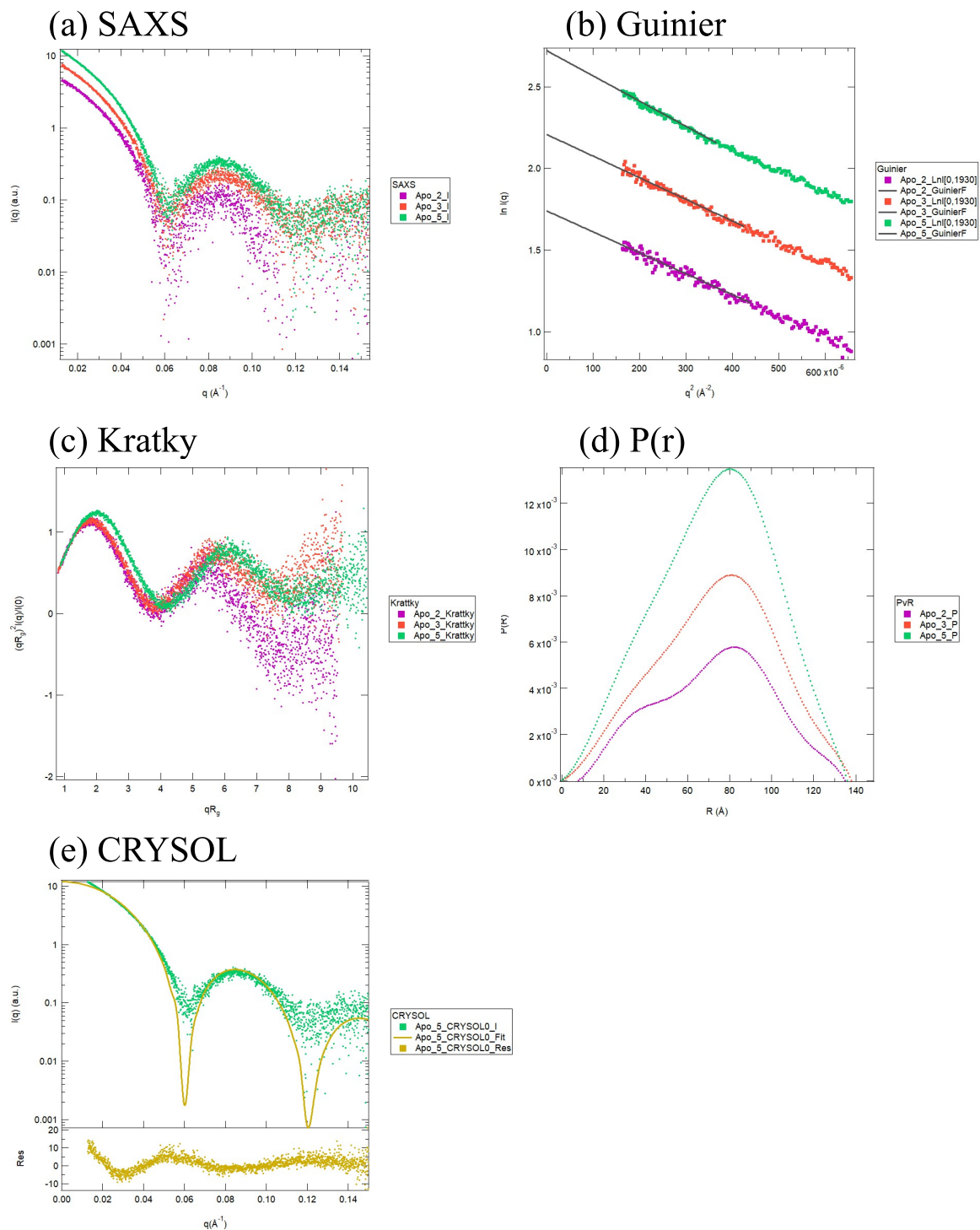

Fig. S6 (a) SAXS patterns of BSA in the concentrations of 2, 3 and 5 mg/ml (green, red and blue, respectively). (b) Guinier plots (black line indicates the fitting). (c) Kratky plots and (d) $P(r)$. (e) Experimental scattering (dots) and the fit from PDB entry 3V03 (solid line).

Fig. S7 (a) SAXS patterns of aldolase in the concentrations of 3 and 5 mg/ml (red and green, respectively). (b) Guinier plots (black line indicates the fitting). (c) Kratky plots and (d) $P(r)$. (e) Experimental scattering (dots) and the fit from PDB entry 1ZAH (solid line).


Fig. S8 (a) SAXS patterns of β-amylase in the concentrations of 2, 3 and 5 mg/ml (green, red and blue, respectively). (b) Guinier plots (black line indicates the fitting). (c) Kratky plots and (d) $P(r)$. (e) Experimental scattering (dots) and the fit from PDB entry 1FA2 (solid line).

Fig. S9 (a) SAXS patterns of Apoferritin in the concentrations of 2, 3 and 5 mg/ml (pink, red and green, respectively). (b) Guinier plots (black line indicates the fitting). (c) Kratky plots and (d) $P(r)$. (e) Experimental scattering (dots) and the fit from PDB entry 1FA2 (solid line).
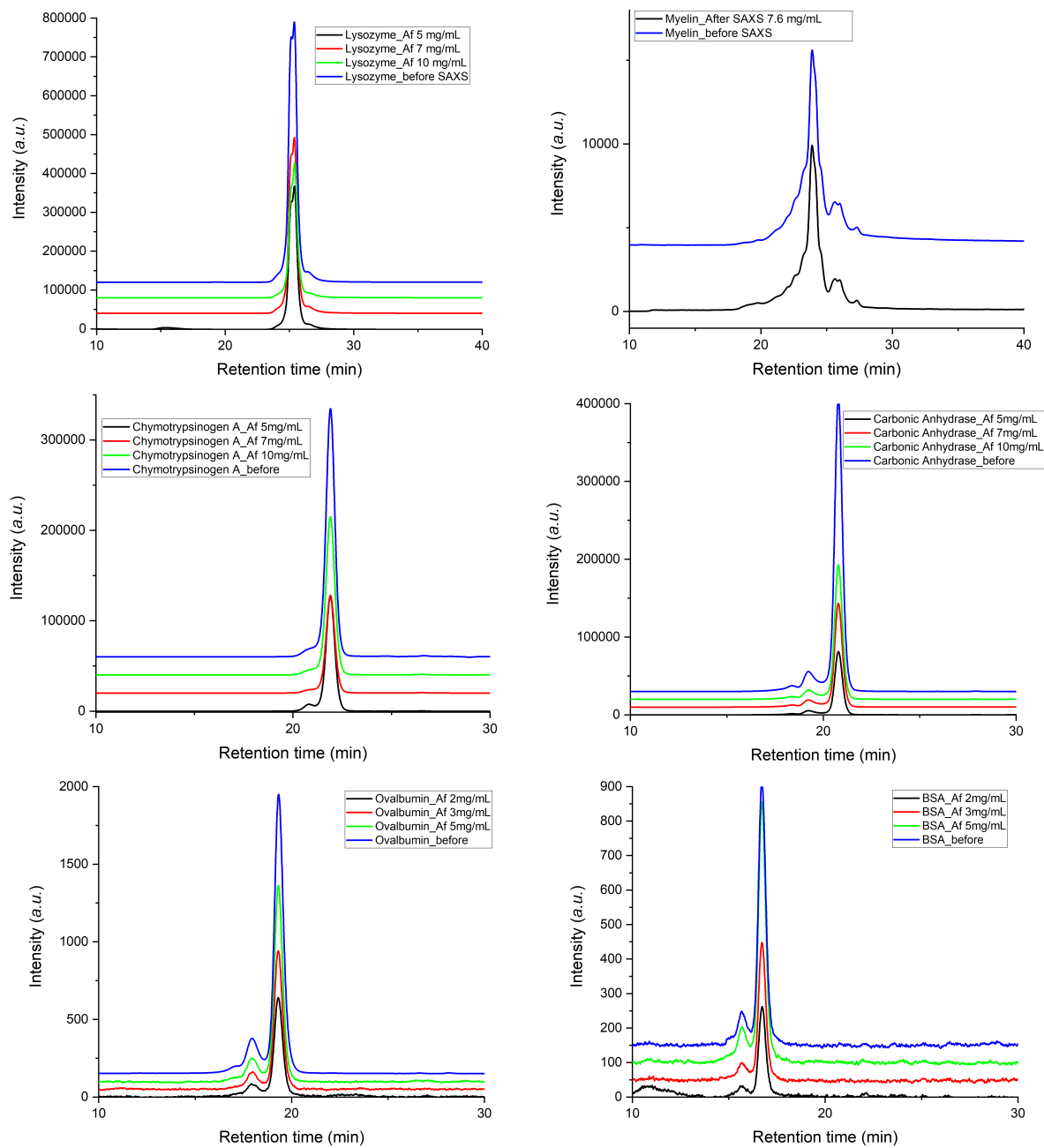
Fig. S10 HPLC chromatograms of lysozyme, MBP, chymotrypsinogen A, carbonic anhydrase, ovalbumin and BSA, respectively. Blueline indicates the protein purity before SAXS experiment while black, red and green are the purity of protein samples after SAXS experiments at the lowest, medium and highest concentrations, respectively.
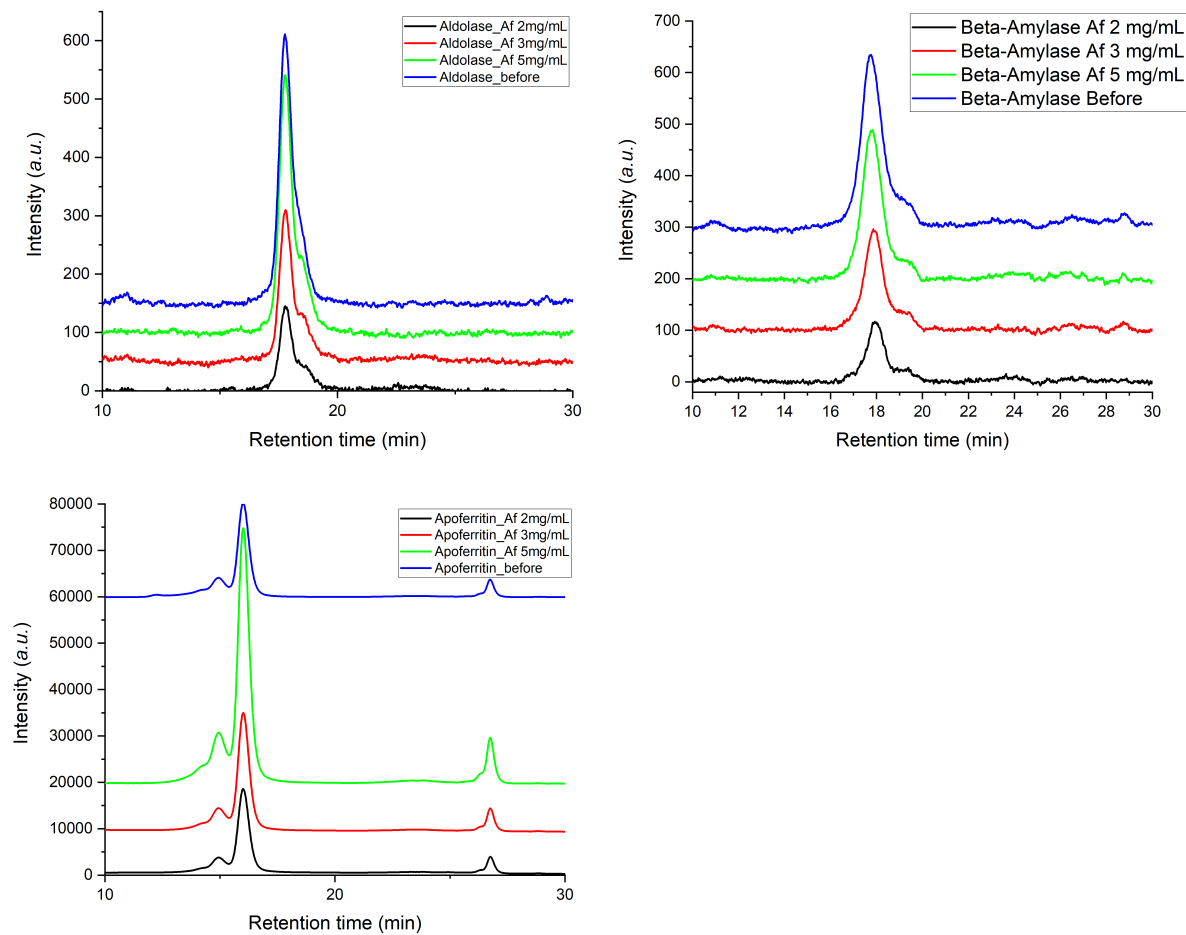
Fig. S11 HPLC chromatograms (continue) of aldolase, β-amylase and apoferritin, respectively. Blueline indicates the protein purity before SAXS experiment while black, red and green are the purity of protein samples after SAXS experiments at the lowest, medium and highest concentrations, respectively.